

DETECTION OF NONLINEARITY IN SEA SURFACE SAR IMAGING PROCESS USING BISPECTRUM METHOD ESTIMATION.

J.M. Le Caillec, R. Garello
Telecom Bretagne, Dpt ITI, BP 832, 29185 Brest Cedex.

B. Chapron
IFREMER, Dpt DRO/OS, BP 70, 29280, Plouzané.

ABSTRACT

Higher order moments have been, for the last decade, an important field of interest, but generally limited to one dimensional signal cases. We introduce in this paper 2D bispectrum to detect nonlinearity in the SAR image mapping process, by using the bicoherency of 2D signal which is theoretically flat over all frequencies, if the process is linear. Two bicoherency estimators are developed, the first one using direct method for bispectral estimation and periodogram for spectral estimator, and the second one based on indirect method and correlogram. In order to validate our nonlinearity detection method, we have tested it first on two simulated images, a linear one and a nonlinear one, and then on two SAR images, one seeming to be nonlinear. Conclusions are drawn by comparing SAR image and simulated image bicoherencies.

Introduction

Parameters extraction and interpretation from Synthetic Aperture Radar (SAR) images of sea surface demonstrate that SAR imaging process involves, in some images, a strong nonlinear mapping process depending on the wave propagation direction, especially in the azimuth direction (i.e. along the satellite track). This will be developed in the first section of this article. Pearson diagram which uses higher order moments has already provided good results in sea surface classification [1]. So the use of higher order spectra (and more especially bispectrum) seems to be interesting in order to detect and quantify nonlinearity in SAR imaging process. The second section of this paper will deal with 2D bispectrum which remains a perspective area, even if some authors have published results of prime importance on this subject. The third section will present results on simulated linear/nonlinear images but also on two typical ERS-1 images one of which seems to be linear and the other one nonlinear.

1. SAR imaging process background

Alpers [2] and Hasselmann [3] pointed out a nonlinear phenomenon in SAR imaging of sea surface. SAR on-board satellites are moving with a constant velocity and send pulses, in a direction perpendicular to the flight path. These pulses are backscattered by the ocean surface and a SAR

image is formed using a Doppler effect (i.e. using backscattered pulse phase information), assumed to be caused by the satellite motion.

Sea surface imaging is more complicated and, because of the ocean shape and motion, Modulation Transfer Functions (MTF) have to be introduced. For instance the "scanning distortion" is caused by wave propagation during the mapping of the image and induces a wavelength rotation. It is nevertheless, neglected for satellite-borne SAR because of the satellite high velocity. The "tilt modulation" takes into account the local incidence angle because SAR does not map directly the sea surface, but the sea slope field, and the spectral wave energy depends on the angle between the normal vector and the incident radar wave number. The "hydrodynamic modulation", the less known of the MTFs, is due to the interaction and energy transport between short waves and long waves.

After applying the last two MTFs a Real Aperture Radar (RAR) image is obtained from the sea surface. These transformations are linear and imply only a multiplication of the original sea surface spectrum by a global transfer function in the frequency domain (and are not specific to the SAR imaging process) whereas the first phenomenon, "velocity bunching", is nonlinear (and is not part of the RAR process). Indeed the orbital velocity of the wave induces a Doppler effect which implies a variation in the backscattered signal phase and so a misplacement of the RAR information in the SAR imaging process.

"Velocity bunching" phenomenon is particularly nonlinear when waves propagate near the azimuth direction. It is so called because pixels are bunched near the wave crest lines. In order to be coherent with models already proposed in one dimensional signal, we proposed a SAR imaging models assuming sea surface to be generated by a linear filter driven by an independent identically distributed noise (i.i.d.). A Pierson-Moscovitz shaped filter may be used and by applying all the MTFs a SAR image process is obtained from an i.i.d. noise passing through a system divided into a linear part and a non linear part as sketched in fig 1.

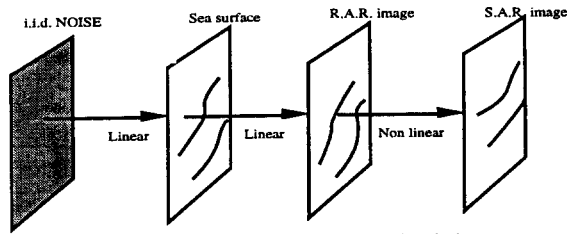


Fig. 1 - 2D SAR imaging process simulation

2. 2D signal bispectrum estimators

Bispectrum of two dimensional signals remains a prospective field of research, due to problems of memory and time computation. Erdem and Tekalp [4] have very well defined the non redundant support of the bispectrum of such signals. Chandran and Elgar [5] have generalized the indirect method of estimation to our case. Third order moment definition of a 2D signal ($X(i, j)$) is given by:

$$M_3^X(n_1, n_2, n_3, n_4) = E\{X(i + n_1, j + n_2) \cdot X(i + n_3, j + n_4) \cdot X(i, j)\}$$

This definition implies only six symmetry relations like in the one dimensional case:

$$\begin{aligned} M_3^X(n_1, n_2, n_3, n_4) &= M_3^X(n_3, n_4, n_1, n_2) = \\ M_3^X(n_3 - n_1, n_4 - n_2, -n_1, -n_2) &= M_3^X(-n_1, -n_2, n_3 - n_1, n_4 - n_2) = \\ M_3^X(n_1 - n_3, n_2 - n_4, -n_3, -n_4) &= M_3^X(-n_3, -n_4, n_1 - n_3, n_2 - n_4) \end{aligned}$$

These six relations are Fourier transformed in a twelve bispectrum classical relation:

$$\begin{aligned} B(\omega_1, \omega_2, \omega_3, \omega_4) &= B^*(-\omega_1, -\omega_2, -\omega_3, -\omega_4) = \\ B(\omega_3, \omega_4, \omega_1, \omega_2) &= B(-\omega_1 - \omega_3, -\omega_2 - \omega_4, \omega_3, \omega_4) = \\ B(-\omega_1 - \omega_3, -\omega_2 - \omega_4, \omega_1, \omega_2) &= B(\omega_1, \omega_2, -\omega_3 - \omega_1, -\omega_4 - \omega_2) \\ &= B(\omega_3, \omega_4, -\omega_3 - \omega_1, -\omega_4 - \omega_2) \end{aligned}$$

One might also generalize the bicoherency definition as:

$$C(\omega_1, \omega_2, \omega_3, \omega_4) = \frac{B(\omega_1, \omega_2, \omega_3, \omega_4)}{\sqrt{S(\omega_1, \omega_2) \cdot S(\omega_3, \omega_4) \cdot S(\omega_1 + \omega_3, \omega_2 + \omega_4)}}$$

A classical result is that the linear system output bicoherency is flat over all frequencies, and we will use this property to estimate the nonlinearity rate in the SAR imaging process. In order to be consistent we have developed the two conventional methods proposed by Nikias [6][7] in the one dimensional case.

In both methods, 256x256 pixel images are segmented into nine 128x128 subimages (with some overlap) with mean subtracted. Then, either the third order moment is computed and a FFT is applied to estimate the bispectrum (it's so called the indirect method with the possible use of special four dimensional windows such as Parzen, Optimal ...), or DFT coefficients are estimated (direct method) and the bispectrum is given by the third order of these coefficients (generally reduced to single produce of three terms).

Image spectrum is also estimated in the same way, by averaging the nine subimage spectra. Contrary to Chandran and Elgar we have added an averaging on the DFT coefficients in the direct method to reduce the estimator

variance. The estimated bispectrum is then included in a 64x64 four dimensional hypercube and the spectrum is also estimated on a 64x64 grid. To avoid incoherent values in bicoherency estimation, especially when spectrum values are almost zero, only points where bicoherency denominator values overpass a certain percentage of the range of denominator values were taken into account. For all the simulations described below, we used values overpassing twenty percent of the denominator one.

3. Simulations and Results.

Our main problem was to visualize information contained in a four dimensional structure and to exploit it. Because we only wanted to detect variations from an assumed constant value, we have, in a first step, detected the most present values in the bicoherency (in fact, the range containing the greater number of bicoherency values). We have in our simulation divide bicoherency ranges into one thousand of equal sub ranges.

In a second step, two variables out of the possible four were fixed and so we defined a plane in the bispectrum. For this plane we have calculated the mean squared error to an assumed constant plane equal to the value the most represented, and we have normalized by this value (this error is then zero if the plane is really constant and equal to the value detected in the step algorithm, i.e. if the process is linear).

This error is mapped in a table at a point which coordinates are given by the frozen variables (for instance if we fixed $\omega_3 = \omega_3^0$ and $\omega_4 = \omega_4^0$, the mean squared error of the plan $B(\omega_1, \omega_2, \omega_3^0, \omega_4^0)$ is mapped at point (ω_1^0, ω_2^0)). Only three tables are built for the three following pairs (ω_1, ω_2) , (ω_1, ω_3) , (ω_2, ω_4) . The other ones can be easily deduced from this three non-redundant tables. In order to test our method and theory we have first simulated two images which are the output of two discrete time filter (a linear one and a quadratic one) having the same non symmetric noise sequence at their input.

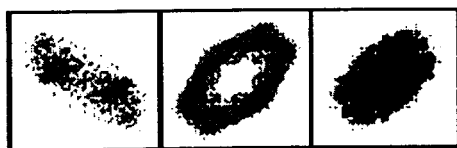
In the first case the output satisfies:

$$Y(k, l) = \sum_{i=1}^I \sum_{j=1}^J a_{i,j} X(k - i, l - j)$$

and for the non linear filter (b being of the same order of magnitude as $a_{i,j}$).

$$Y(k, l) = \sum_{i=1}^I \sum_{j=1}^J a_{i,j} \cdot X(k - i, l - j) + b \cdot X(k, l) \cdot X(k, l)$$

Results presented below are normalized mean squared error (NMSE) tables drawn by logarithmic level, the darker is the point, the greater is the error. We used a 63 points centered window size, in the indirect method to estimate the third order moment, and a 5 points window to average DFT coefficients.



linear image tables estimated by direct method



linear image tables estimated by indirect method

A first comparison between both estimators indicates a greater error in the indirect method caused perhaps by a greater variance of this estimator. But generally, these estimators give very similar results. The same conclusion is reached for the quadratic filter case.



nonlinear image tables estimated by direct method



nonlinear image tables estimated by indirect method

In both cases, adding a quadratic term has increased the NMSE (tables are darker), the direct method seeming more selective. But more especially we can find a tiny peak, where the NMSE is very high. In the table slices (passing through the maximum of each table) below, for both estimators, we can distinguish this peak and we consider to have detected incoherency.

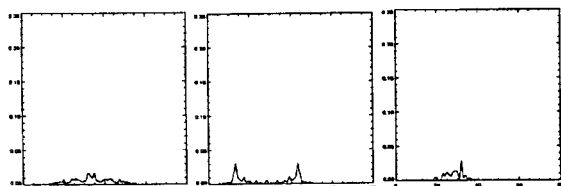


table slices for linear image and direct method

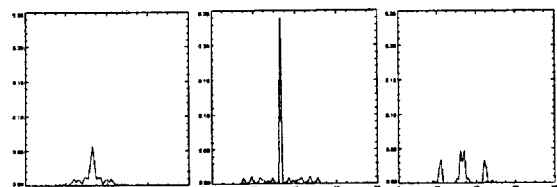


table slices for non linear image and direct method

Table slices obtained with indirect method give very similar results.

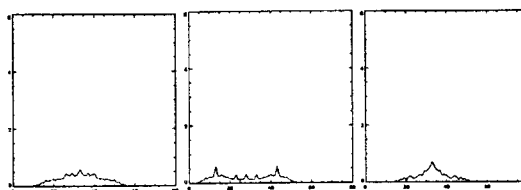


table slices for linear image and indirect method

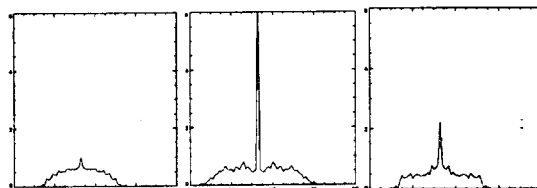
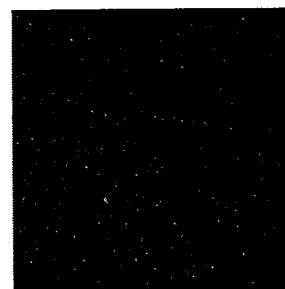
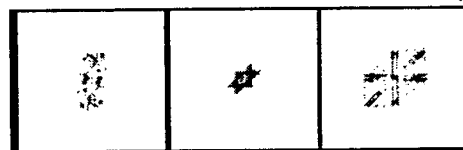


table slices for nonlinear image and indirect method

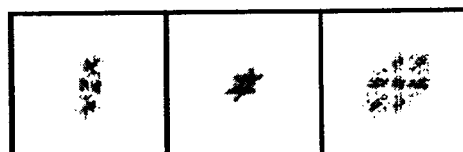
We can consider to have a tool for detecting nonlinearities. More complicated nonlinear systems could provide very different tables and different "incoherency" peak localizations (not visible in linear image tables). For SAR images we chose two typical images. On the upper one we can see waves propagating in the azimuth direction whereas no waves can be distinguished on the lower image.



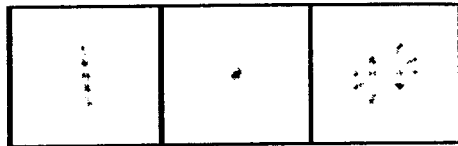
The NMSE tables are presented below:



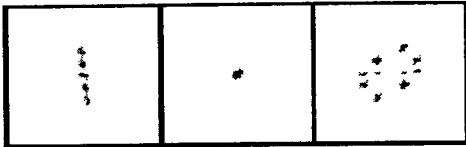
"linear" image tables estimated by direct method



"linear" image tables estimated by indirect method



"non linear" image tables estimated by direct method.



"non linear" image tables estimated by indirect method.

Results obtained from both method are very similar also. The main differences between the two sets of tables lie in the way an "incoherency" peak appears for the second image as shown in table slices below.

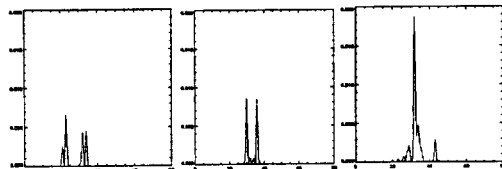


table slices for "linear" image and direct method

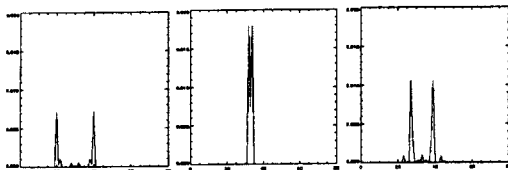


table slices for "non linear" image and direct method

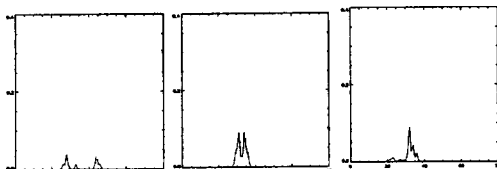


table slices for "linear" image and indirect method

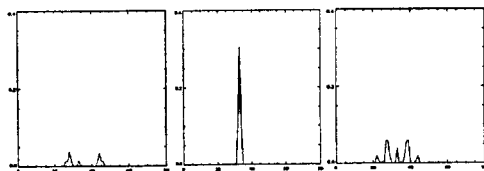


table slices for "non linear" image and indirect method

At the exception of one bicoherency table given by the direct method for "linear" image showing an unexplained strong "incoherency" peak, we can observe similar behavior between the bicoherency of simulated images and the bicoherency of SAR images. This indicates a stronger nonlinear process in the second image as expected, but doesn't imply that nonlinear processes are not involved in first image mapping process.

Conclusion.

In this paper, we have shown the possibility to discriminate SAR images for which the mapping process induces nonlinearities. However more theoretical works and comparisons with identified cases of nonlinearities are necessary to fully understand all the implications of the results found. Some important results remain to be established, in particular the strength of the non linearity (if we can separate in a linear and a nonlinear filter, it would be interesting to know the energy due to each part), or as in our case if nonlinearity are "oriented" along one special axis, what is the tables behavior. Some improvement must concern the robustness of such methods to avoid incoherent value as we have found for the linear method.

Finally, comparisons with bicepstrum results for linear process [8] would be interesting to perform. However, as for bicoherency estimation, the main problem lies in the extraction of information contained in a four dimensional bicepstrum.

References:

- [1] Delignon Y., R. Garelo, A. Hillion, "Parameterisation of Sea State from SAR Images", ICASSP 92 - pp. III. 29-32.
- [2] Alpers, W.R. and C.L. Rufenach, 1979. The Effect of Orbital Motions on Synthetic Aperture Radar Imagery of Ocean Waves. *IEEE Transactions on Antennas and Propagation*, vol. AP-27, no 5, pp. 685-689.
- [3] Hasselmann K., S. Hasselmann, "On the Nonlinear Mapping of an Ocean Surface Wave Spectrum and its Inversion" *J.G.R.*, 96(c6), 1991 pp. 10713-10729.
- [4] Tekalp A.M., A.T. Erdem, "New Theoretical Results on the Bistatistics of 2-D Signal", *Higher-order statistics*, J.L. Lacoue Ed., pp. 99-102.
- [5] Chandran V., S. Elgar, "Bispectral Analysis of Two-Dimensional Random Processes", *I.E.E.E. Transaction on ASSP*, vol. 38, n° 12, Dec. 1990, pp. 2181-2186.
- [6] Nikias C.L., J.M. Mendel, "Signal Processing With Higher-Order Spectra", *I.E.E.E Signal Magazine*, July 1993.
- [7] Nikias C.L., A.P. Petropulu, *Higher-Order Spectra Analysis, A nonlinear signal processing framework*, Prentice Hall.
- [8] Tekalp A.M., A.T. Erdem, "Higher-Order Spectrum Factorization in One and Two Dimensions and Application in Signal Modeling and Nonminimum Phase System Identification", *I.E.E.E. Transaction on ASSP*, vol. 37, n° 10, Oct. 1989, pp. 1537-1549.